

Motivation

Status quo

- Gaining a microscopic understanding of the effect of strong electron-phonon interactions remains a challenge to theory.
- Recently, numerical calculations revealed new phenomena such as the emergence of nontrivial phases with broken symmetry or the existence of several hydrodynamic regimes [1].

Aim

- Study the Holstein model (simple model describing electron-phonon interactions in condensed matter) with renormalization group (RG) methods to obtain a deeper understanding of the nature of phase transitions.

Holstein model [2]

$$\mathcal{H} = \sum_k \epsilon_k c_k^\dagger c_k + \omega_0 \sum_q b_q^\dagger b_q + \frac{\gamma_0}{\sqrt{V}} \sum_{k,q} c_{k+q}^\dagger c_k X_q \quad (1)$$

- dispersionless Einstein phonons with frequency ω_0
- strength of electron-phonon coupling is given by $\lambda_0 = \nu\gamma_0^2/\omega_0^2$

Migdal's theorem [3]

Vertex corrections can be neglected even for large electron-phonon interaction λ_0 as long as

$$\lambda_0 \omega_0 / \epsilon_F \ll 1 \quad (2)$$

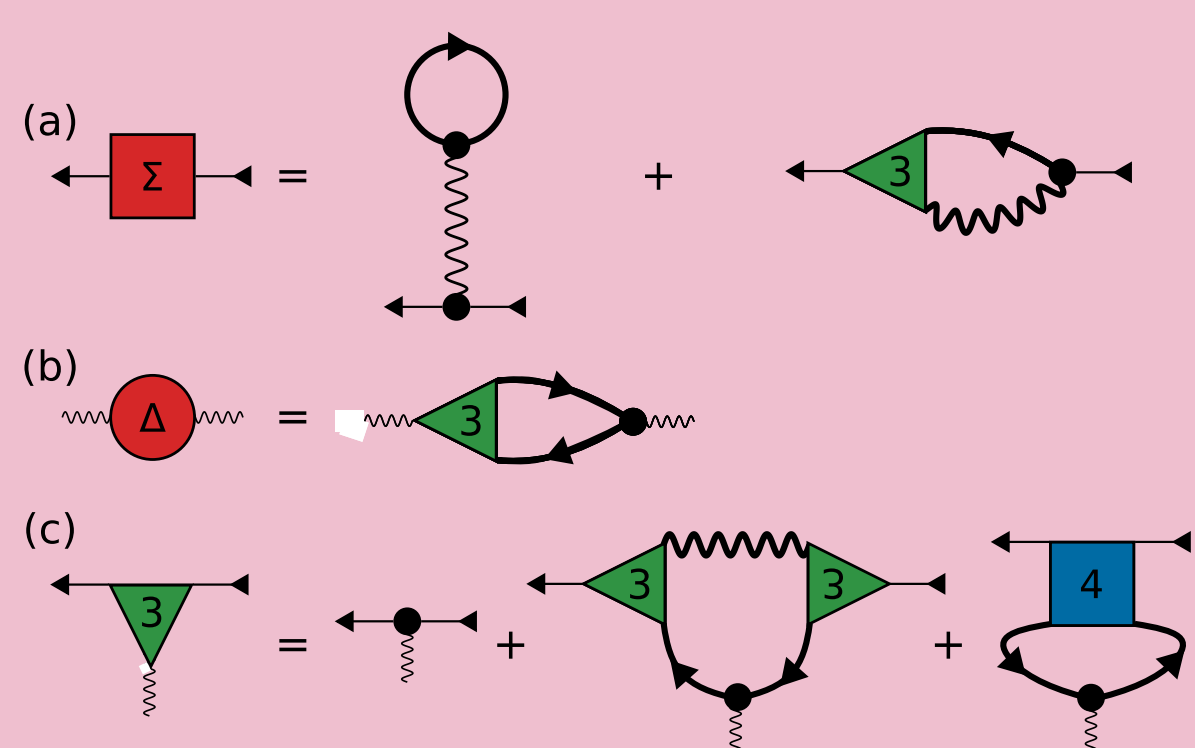
(based on a perturbative calculation of the leading-order correction to the electron-phonon vertex).

- Recently, numerical evidence has been presented [4] that in the two-dimensional Holstein model this generally accepted scenario may not be valid when λ_0 is of order unity.

Pomeranchuk Instability and QCP

Ward identities

Dyson-Schwinger equations



FRG equation with μ as flow parameter

$$\frac{\partial \Sigma(K)}{\partial \mu} = \Gamma^{\bar{c}c\varphi}(K, K, 0) \frac{\partial \phi^0}{\partial \mu} - I(K),$$

where

$$I(K) = \int_{K'} G^2(K') [\Gamma^{\bar{c}c\bar{c}c}(K, K', K', K) + \Gamma^{\bar{c}c\varphi}(K, K', K - K') D(K' - K) \times \Gamma^{\bar{c}c\varphi}(K', K, K' - K)].$$

- We obtain the following Ward identity:

$$\frac{\Gamma^{\bar{c}c\varphi}(K, K, 0)}{\gamma_0} = \frac{1 - \frac{\partial \Sigma(K)}{\partial \mu}}{1 - \frac{\Sigma_p}{\partial \mu}} = \frac{1 - \frac{\partial \Sigma(K)}{\partial \mu}}{1 - \frac{\gamma_0^2 \partial \rho}{\omega_0^2 \partial \mu}}, \quad (3)$$

relating the electron-phonon vertex to the derivative of the electronic self-energy with respect to μ

- and the compressibility sum rule

$$\frac{\partial \rho}{\partial \mu} \equiv \frac{\partial}{\partial \mu} \int_K G(K) = \frac{\Pi(0)}{1 - \gamma_0^2 D_0(0) \Pi(0)}, \quad (4)$$

where $\Pi(Q) = -\Delta(Q)/\gamma_0^2$ is the irreducible polarization. From this it is easy to show that for $Q = 0$ the inverse phonon propagator is given by

$$D^{-1}(0) = \omega_0^2 + \Delta(0) = \frac{\omega_0^2}{1 + \frac{\gamma_0^2 \partial \rho}{\omega_0^2 \partial \mu}}. \quad (5)$$

- Thermodynamic stability implies that the compressibility is non-negative and thus $D^{-1}(0) \geq 0$. This also means that the compressibility diverges when the renormalized phonon frequency vanishes!

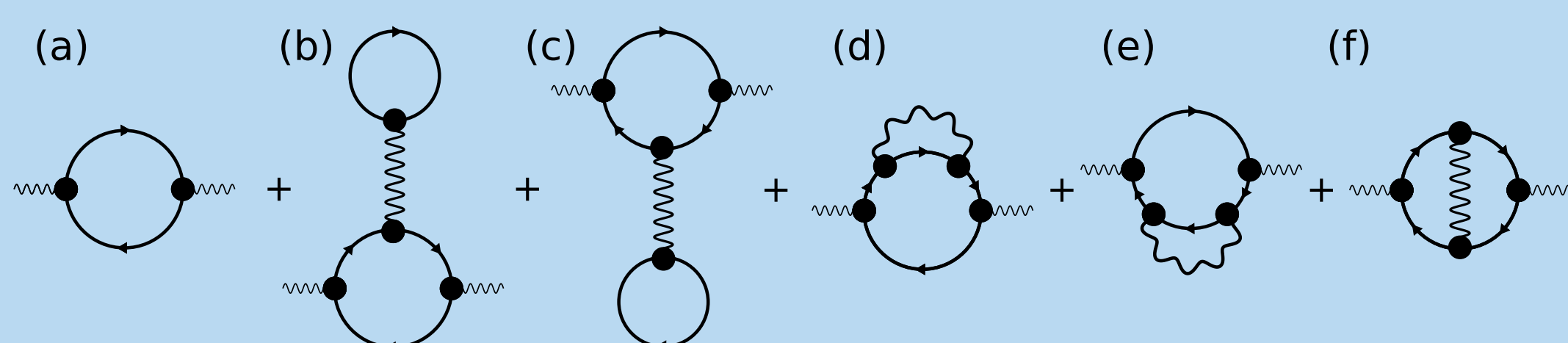
Perturbation Theory & Effective Phonon Action

Renormalized phonon frequency

The square of the renormalized phonon frequency to second order in λ_0 is given by

$$\tilde{\omega}_0^2 = \omega_0^2 \left[1 - \lambda_0 - \frac{4}{3} \lambda_0^2 + \mathcal{O}(\lambda_0^3, \lambda_0^2 \omega_0 / \epsilon_F) \right]. \quad (6)$$

where we evaluated the following diagrams



- For $\lambda_c = \frac{\sqrt{57}-3}{8} \approx 0.57$ the renormalized phonon frequency vanishes. The compressibility sum rule then implies a divergent compressibility. At this point the system exhibits a Pomeranchuk instability in the zero angular momentum density channel associated with phase separation [5].

- However λ_c is of $\mathcal{O}(1)$ so higher orders cannot be neglected. At this point we cannot exclude that higher orders in λ_0 remove the Pomeranchuk instability so we use the nonpert. FRG in the following.

Effective phonon action

Since we are only interested in the renorm. phonon frequency we can integrate out the electrons to obtain

$$S_{\text{eff}}[X] = \frac{1}{2} \int_Q D_0^{-1}(Q) X_{-Q} X_Q - \text{Tr} \ln [1 - G_0 X]. \quad (7)$$

By expanding the logarithm we see that the interaction vertices are given by the symmetrized closed fermion loops, meaning that the inverse propagator, shown in Eq. (14), is by the RPA result.

Functional Renormalization Group Approach

A. Exact flow equations for the average effective phonon action

Introduction of the Regulator

$$S_\Lambda[X] = S_{\text{eff}}[X] + \frac{1}{2} \int_Q R_\Lambda(Q) X_{-Q} X_Q \quad (8)$$

Wetterich equation [6]

$$\partial_\Lambda \Gamma_\Lambda[\phi] = \frac{1}{2} \text{Tr} \left[(\Gamma_\Lambda''[\phi] + R_\Lambda)^{-1} \partial_\Lambda R_\Lambda \right] \quad (9)$$

The phonon field ϕ has a finite expectation value. Usually, one would introduce a scale dependent expectation value and appropriately chosen fluctuations for example through

$$\phi = \phi_{\Lambda, Q}^0 + \varphi_Q. \quad (10)$$

However, this expectation value is related to the electron density ρ via the Dyson-Schwinger equation

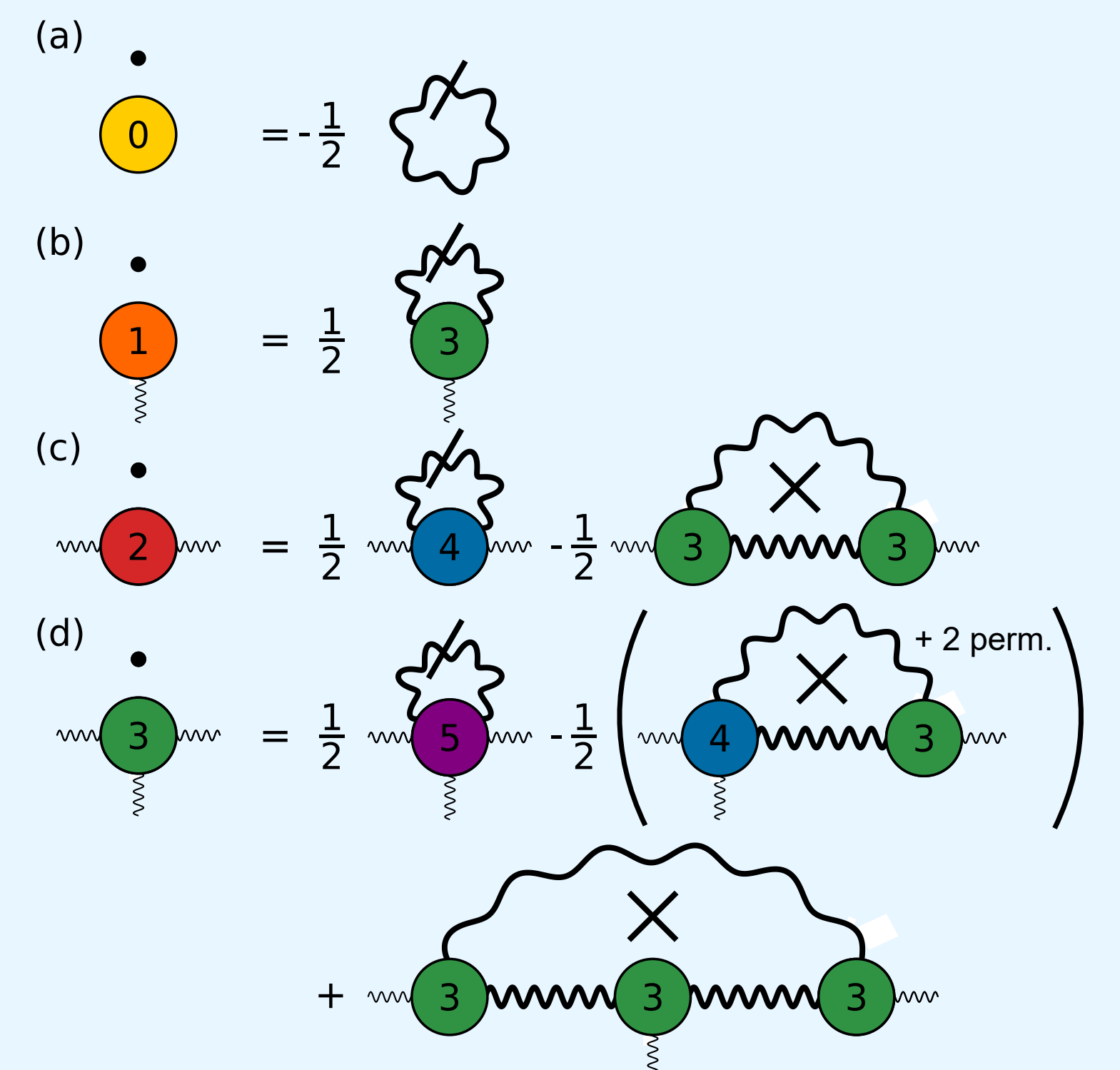
$$\phi^0 = -\gamma_0 D_0^{-1}(0) \int_K G(K) = -\frac{\gamma_0}{\omega_0^2} \rho. \quad (11)$$

In order to keep ρ constant during the flow we expand around ϕ^0 , introducing

$$\tilde{\Gamma}_\Lambda[\varphi] = \Gamma_\Lambda[\phi^0 + \varphi], \quad (12)$$

with the boundary condition

$$\lim_{\Lambda \rightarrow 0} \tilde{\Gamma}_\Lambda^{(1)} = 0. \quad (13)$$



B. Classification of couplings and flow of relevant couplings

$$\tilde{\Gamma}_\Lambda^{(2)}(Q) = r_0 + b_0 \frac{|\bar{\omega}|}{q} + c_0 q^2 + \mathcal{O}(\bar{\omega}^2, q^4) \xrightarrow{\text{Assume}} \tilde{\Gamma}_\Lambda^{(2)}(Q) = r_\Lambda + b_\Lambda \frac{|\bar{\omega}|}{q} + c_\Lambda q^2 + \mathcal{O}(\bar{\omega}^2, q^4) \quad (14)$$

Choice of dynamical exponent z

$$q \propto \Lambda \quad (15a)$$

$$\bar{\omega} \propto \Lambda^z \quad (15b)$$

$$\phi_Q \propto \Lambda^{-\frac{d+z}{2}} \quad (15c)$$

Set the dynamical exponent $z = 3$. Therefore, the flow of b_Λ and c_Λ are marginal, $\tilde{\Gamma}^{(4)}$ irrelevant $\rightarrow d_{\text{eff}} = d + z = d + 3$.

$$h_\Lambda = \tilde{\Gamma}_\Lambda^{(1)} \propto \Lambda^{-\frac{d+5}{2}} \quad (16a)$$

$$r_\Lambda = \tilde{\Gamma}_\Lambda^{(2)}(0) \propto \Lambda^{-2} \quad (16b)$$

$$g_\Lambda = \tilde{\Gamma}_\Lambda^{(3)}(0, 0, 0) \propto \Lambda^{-\frac{d-3}{2}} \quad (16c)$$

C. RG flow and Pomeranchuk fixed points in $d > 3$

Only retaining all relevant vertices the flow equations are

$$\partial_\Lambda h_\Lambda = \frac{g_\Lambda}{2} \int_Q \tilde{D}_\Lambda(Q), \quad (17a)$$

$$\partial_\Lambda r_\Lambda = -g_\Lambda^2 \int_Q \tilde{D}_\Lambda(Q) \tilde{D}_\Lambda(Q), \quad (17b)$$

$$\partial_\Lambda g_\Lambda = 3g_\Lambda^3 \int_Q \tilde{D}_\Lambda(Q) \tilde{D}_\Lambda^2(Q). \quad (17c)$$

By choosing a Litim [7] type regulator, adapted to Eq. (14),

$$R_\Lambda(Q) = (c_0 \Lambda^2 - b_0 |\bar{\omega}|/q - c_0 q^2) \Theta(c_0 \Lambda^2 - b_0 |\bar{\omega}|/q - c_0 q^2), \quad (19)$$

all integrals entering the flow equations [17a-17c] become analytically manageable, leading to the system of (rescaled) ordinary differential equations [20a-20c].

Rescaled flow equations

$$\partial_t \tilde{h}_t = \frac{d+5}{2} \tilde{h}_t + \frac{\tilde{g}_t}{(\tilde{r}_t+1)^2} \quad (20a)$$

$$\partial_t \tilde{r}_t = 2\tilde{r}_t - \frac{\tilde{g}_t^2}{(\tilde{r}_t+1)^3} \quad (20b)$$

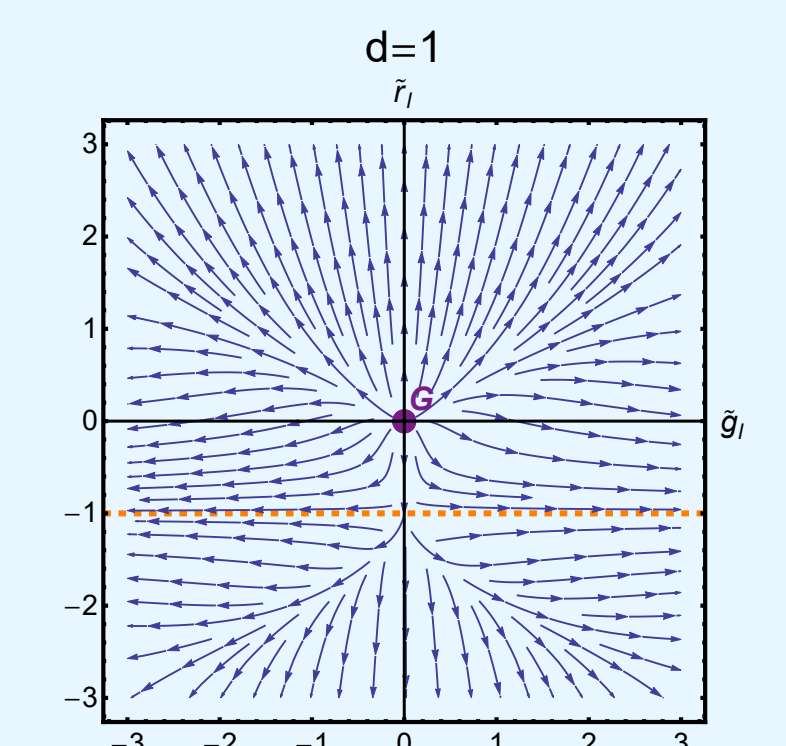
$$\partial_t \tilde{g}_t = \frac{3-d}{2} \tilde{g}_t + \frac{3\tilde{g}_t^3}{(\tilde{r}_t+1)^4} \quad (20c)$$

Eq. (20c) only has fixed points for $d > 3$, leading to two nontrivial Pomeranchuk fixed points P^\pm for $d = 4$ and none for $d \leq 3$. Linearization of the flow equations around the fixed points P^\pm shows that both are **tricritical**.

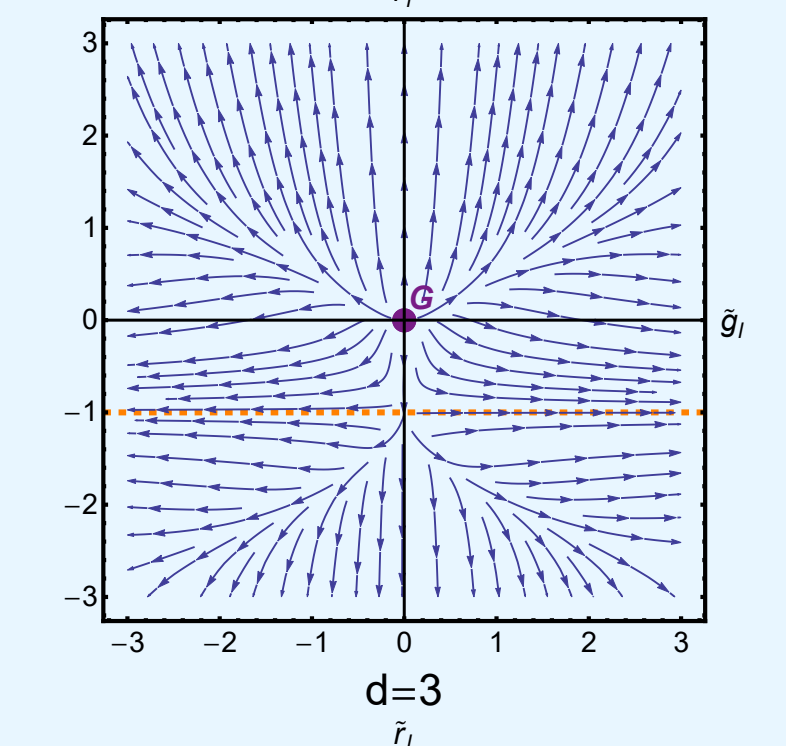
Reg. phonon propagator

$$\tilde{D}_\Lambda(Q) = \frac{1}{\tilde{\Gamma}_\Lambda^{(2)}(Q) + R_\Lambda(Q)} \quad (18)$$

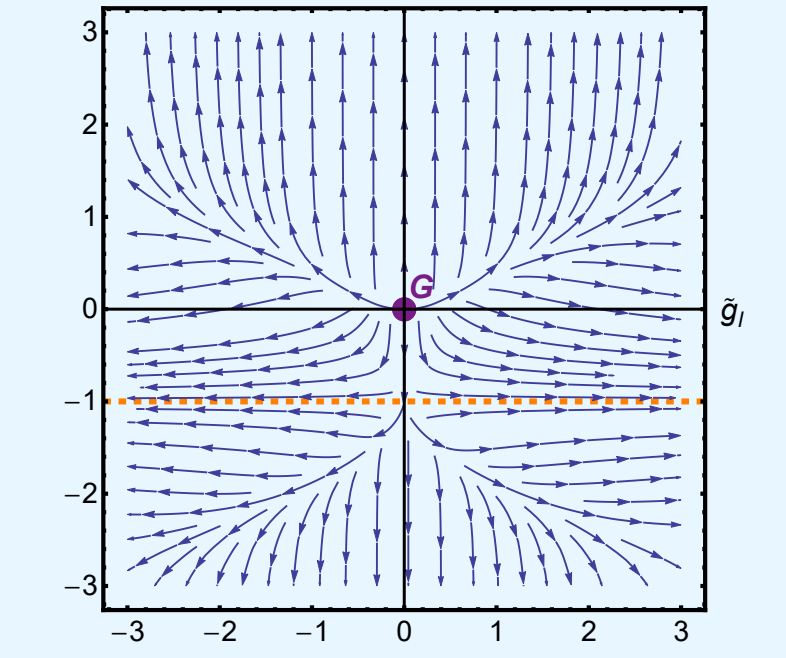
d=1



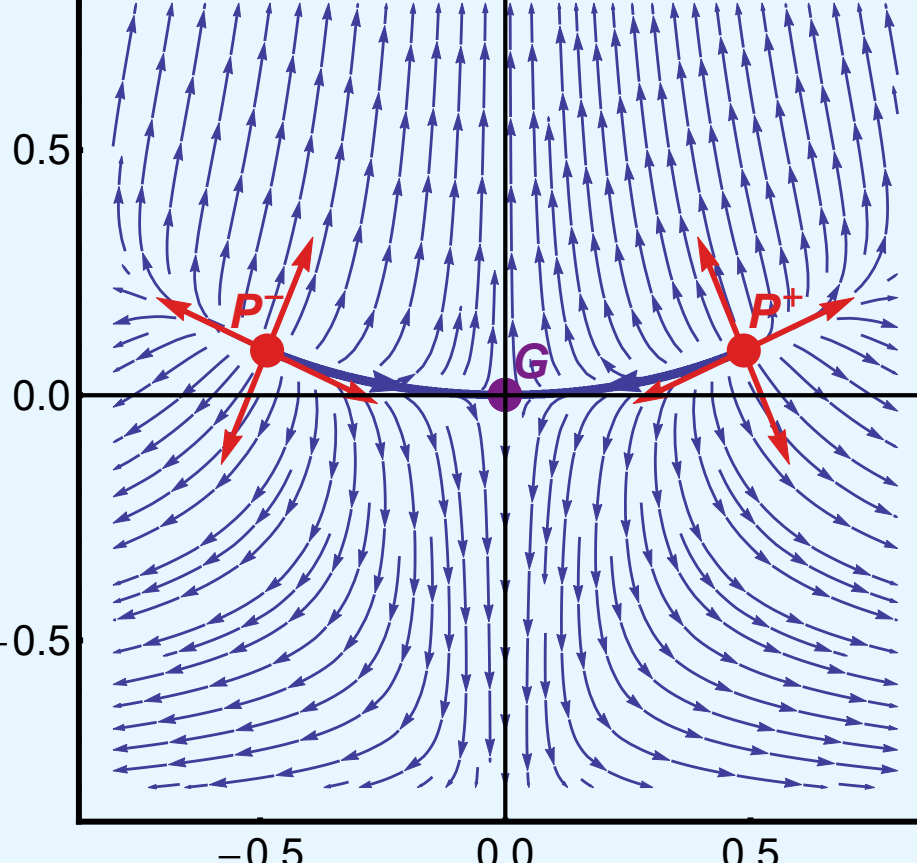
d=2



d=3



d=4



-0.5 0.0 0.5

0.5

0.0

-0.5

-1.0

-1.5

-2.0

-2.5

-3.0

-3.5

-4.0

-4.5

-5.0

-5.5

-6.0

-6.5

-7.0

-7.5

-8.0

-8.5

-9.0

-9.5

-10.0

-10.5

-11.0

-11.5

-12.0

-12.5

-13.0

-13.5

-14.0

-14.5

-15.0

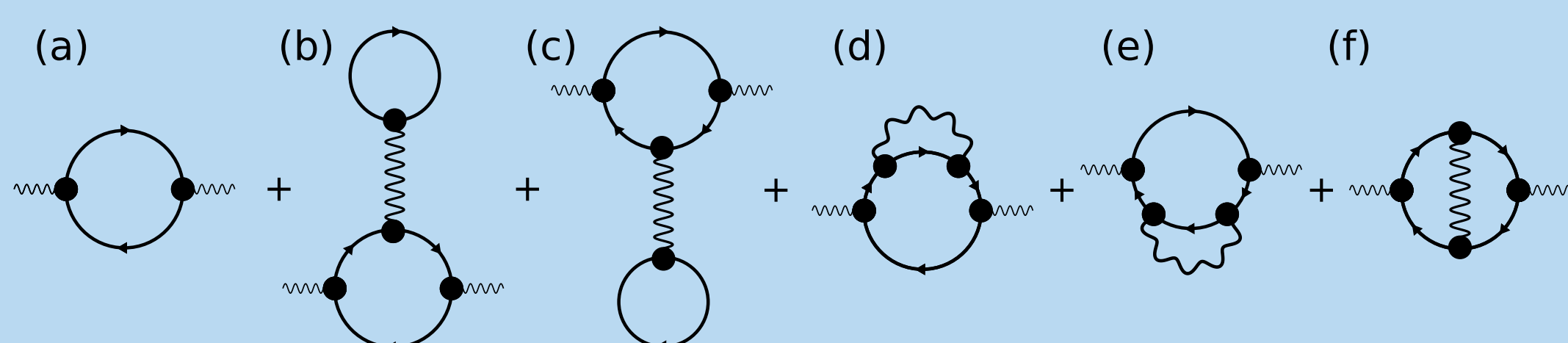
Perturbation Theory & Effective Phonon Action

Renormalized phonon frequency

The square of the renormalized phonon frequency to second order in λ_0 is given by

$$\tilde{\omega}_0^2 = \omega_0^2 \left[1 - \lambda_0 - \frac{4}{3} \lambda_0^2 + \mathcal{O}(\lambda_0^3, \lambda_0^2 \omega_0 / \epsilon_F) \right]. \quad (6)$$

where we evaluated the following diagrams



- For $\lambda_c = \frac{\sqrt{57}-3}{8} \approx 0.57$ the renormalized phonon frequency vanishes. The compressibility sum rule then implies a divergent compressibility. At this point the system exhibits a Pomeranchuk instability in the zero angular momentum density channel associated with phase separation [5].

- However λ_c is of $\mathcal{O}(1)$ so higher orders cannot be neglected. At this point we cannot exclude that higher orders in λ_0 remove the Pomeranchuk instability so we use the nonpert. FRG in the following.

Effective phonon action

Since we are only interested in the renorm. phonon frequency we can integrate out the electrons to obtain

$$S_{\text{eff}}[X] = \frac{1}{2} \int_Q D_0^{-1}(Q) X_{-Q} X_Q - \text{Tr} \ln [1 - G_0 X]. \quad (7)$$

By expanding the logarithm we see that the interaction vertices are given by the symmetrized closed fermion loops, meaning that the inverse propagator, shown in Eq. (14), is by the RPA result.

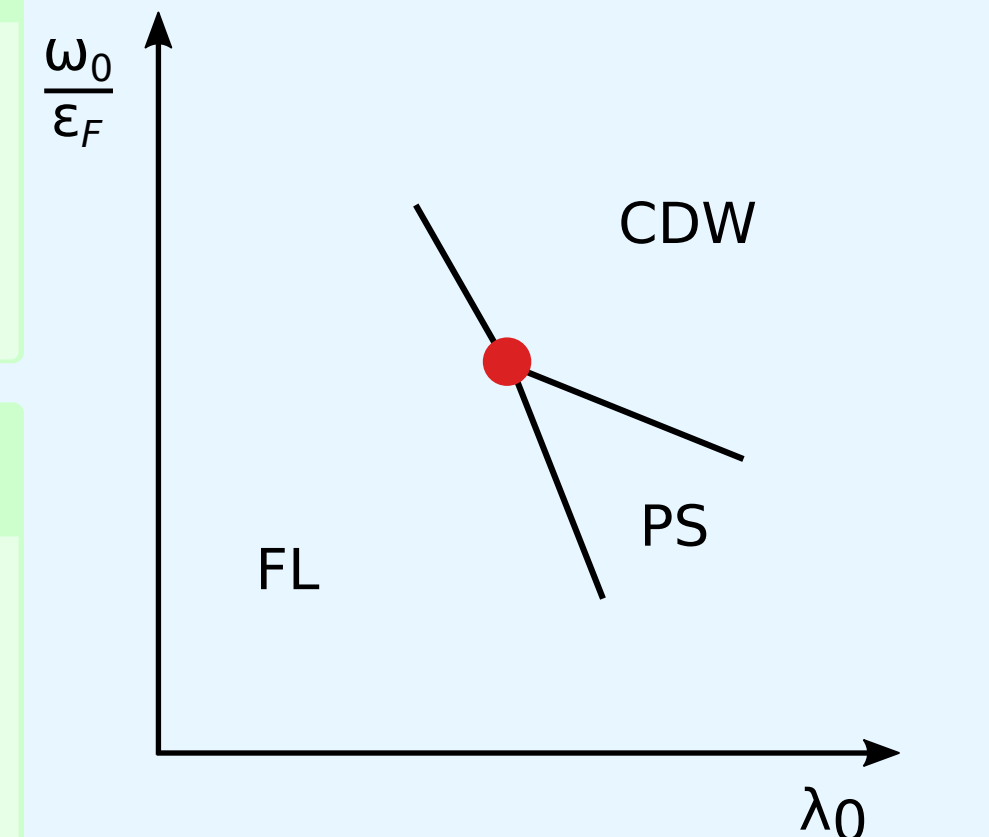
Conclusions

Schematic phase diagram [4]

Since we ignored a possible superfluid phase the weak-coupling phase is a Fermi Liquid. For $d \leq 3$ we do expect a first-order transition to a phase separation for $\lambda_0 \sim \mathcal{O}(1)$, while the adiabatic limit is expected to feature a charge-density-wave phase.

Connection to ϕ^3 -theory in $d > 6$

Since $d_{\text{eff}} = d + 3$ the P^\pm are related to the nontrivial ultraviolet-stable fixed point of ϕ^3 -theory in above six dimensions. Those are of interest in high energy physics, because they offer a possibility to construct a well-defined continuum limit of perturbatively non-renormalizable field theories (asymptotic safety scenario).



References

- S. Kumar and J. van den Brink, Phys. Rev. B **78**, 155123 (2008). Y. Murakami et al., Phys. Rev. Lett. **113**, 266404 (2014). T. Ohgoue and M. Imada, Phys. Rev. Lett. **119**, 197001 (2017). Y. Wang et al., Phys. Rev. Res. **2**, 043258 (2020). X. Huang and A. Lucas, Phys. Rev. B **103**, 155128 (2021).
- T. Holstein, Ann. Phys. (NY) **8**, 325 (1959).
- A. B. Migdal, Zh. Eksp. Teor. Fiz. **34**, 1438 (1958) [Sov. Phys. JETP **7**, 996 (1958)].
- I. Esterlis et al., Phys. Rev. B **97**, 140501 (R) (2018). I. Esterlis, S.A. Kivelson, and D.J. Scalapino, Phys. Rev. B **99**, 174516 (2019). A.V. Chubukov, A. Abanov, I. Esterlis, and S.A. Kivelson, Ann. Phys. **417**, 168190 (2020).
- A. V. Chubukov, A. Klein, and D. L. Maslov, J. Exp. Theor. Phys. **127**, 826 (2018)
- C. Wetterich, Phys. Lett. B **301**, 90 (1993). P. Kopietz, L. Bartosch, and F. Schütz, (Springer, Berlin, 2010). N. Dupuis, L. Canet, A. Eichhorn, W. Metzner, J. M. Pawłowski, M. Tissier, and N. Wschebor, Phys. Rep. **910**, 1 (2021). And many more.
- D. F. Litim, Phys. Rev. D **64**, 105007 (2001).